Corbino geometry Josephson junction

Robert H. Hadfield,* Gavin Burnell, Dae-Joon Kang, Chris Bell, and Mark G. Blamire
Interdisciplinary Research Centre in Superconductivity and Department of Materials Science, University of Cambridge, Pembroke Street, CB2 3QZ Cambridge, United Kingdom

(Received 1 August 2002; revised manuscript received 8 January 2003; published 24 April 2003)

We report the fabrication and measurement of Corbino geometry superconductor–normal metal–superconductor Josephson junctions. A circular junction barrier is defined in a superconductor–normal metal bilayer and bias current flows through the device in the radial direction. In contrast to conventional junction geometries, the junction barrier is entirely surrounded by a superconducting loop: this implies that flux can enter the junction only as single quanta. We have observed abrupt suppression/reappearance of critical current corresponding to flux entry/annihilation events as the external magnetic field is varied. Furthermore, when the width of the superconducting film enclosing the junction is sufficiently small we observe critical current suppression/reappearance in a series of jumps, suggesting incomplete quantization of magnetic flux in a superconducting film over mesoscopic length scales. We present a theoretical simulation of device response to the approach of a single vortex. A consideration of the actual device geometry shows that screening currents in the edge of the film when an external magnetic field is applied to a bilayer strip containing the junction create an effective double-well potential for confined flux vortices trapped in the junction. Further experiments and possible applications of such devices are discussed.

DOI: 10.1103/PhysRevB.67.144513 PACS number(s): 74.50.+r

I. INTRODUCTION

The unique properties of infinite (circular) barrier Josephson junctions have long been recognized.[1–3] Early attempts were made to fabricate cylindrical superconductor-insulator-superconductor (SIS) junctions by thin-film deposition on top of a wire.[4,5] Recent experimental work has focused on nonideal geometries that can be realized using conventional microfabrication techniques. An annular SIS junction is formed when a conventional planar SIS tunnel junction is patterned into a ring, yielding a high quality circular barrier of carefully controlled dimensions. The properties of annular SIS junctions with and without trapped fluxons are now extremely well understood.[6–10] Quantized flux can be trapped around one electrode and the overall field in the junction barrier can be modulated by the application of an in-plane magnetic field. Due to the underdamped conditions, soliton motion of fluxons up to superluminal velocities can be achieved. Such junctions are of interest both for detector applications and for fundamental studies.[11,12] However, in the annular geometry, some of the most interesting properties predicted for circular junctions, such as Berry phase effects,[13,14] cannot be observed.

In this paper, we report on the first thin-film based junction with the circular barrier in the same plane as the electrodes. This is an extension of our established focused ion beam (FIB) based planar superconductor–normal metal–superconductor (SNS) junction fabrication technique. The starting point is a superconductor–normal-metal bilayer. A 50 nm wide trench is milled into the upper superconducting layer in order to achieve weak coupling. By milling a circular trench and making an electrical contact to the central island, we arrive at a Corbino geometry SNS junction. The term is derived from the experiment carried out by Corbino in 1911 to demonstrate the Hall effect in a disk-shaped conducting sample.[15]

A simple consideration of the basic phenomenology we may expect in this special junction geometry is illustrated in Fig. 1. In a conventional Josephson junction magnetic flux can enter progressively through the edges of the junction. As a result the phase difference between the electrodes varies across the width of the junction, leading to a continuous modulation of the junction critical current. In the simplest two-dimensional geometry the critical current versus magnetic field, $I_C(B)$, follows a modulus of a sinc function dependence, analogous to the diffraction pattern of monochromatic light due to a single slit in the Fraunhofer regime.[16] The first minimum occurs when one flux quantum Φ_0 is present in the barrier. In the case of a SNS junction fabricated in the Corbino geometry, the barrier region is entirely enclosed in a loop of superconductor, therefore magnetic flux is only permitted to enter as single quanta.[1] The critical current versus magnetic-field dependence $[I_C(B)]$ should now abruptly switch from the maximum value to zero as flux

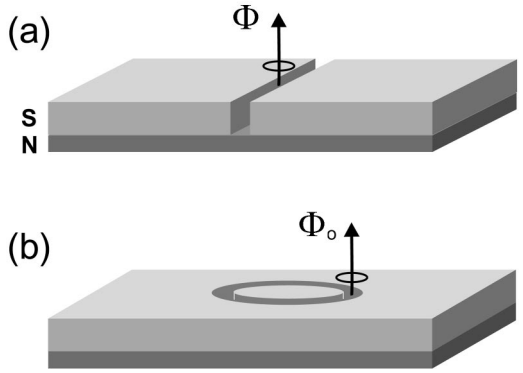

FIG. 1. Schematic of flux entry into different Josephson junction geometries. (a) Conventional junction geometry (planar SNS bridge): flux enters freely through sides of junction leading to Fraunhofer-like critical current response. (b) Corbino geometry junction: flux can only enter as quantized vortices, hence we may expect an abrupt critical current suppression when a vortex enters the junction.

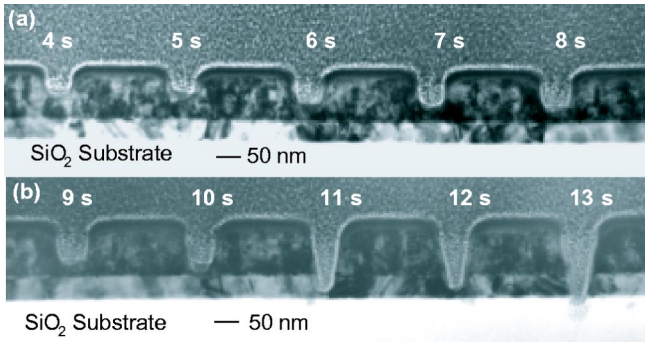

FIG. 2. Bright field TEM images of a series of cuts in a 125 nm Nb 50 nm bilayer track. Milling times are indicated. Area milled $=2.5\ \mu\text{m}\times 50$ nm.

enters, resulting in a top hat $I_C(B)$ pattern. In this paper we report primarily on the response $I_C(B)$ of such junctions at 4.2 K—as we shall see, the observed behavior is more subtle than this simple picture. As the junction is overdamped, quantized flux trapped in the barrier will not propagate freely. However, when a bias current is applied, the flux can be driven around the barrier. In the low-temperature limit the driving force should be attenuated by Berry phase effects.[14,17]

II. EXPERIMENTAL TECHNIQUE

A. Planar SNS junction fabrication by focused ion beam

We give here a brief summary of FIB planar SNS device fabrication; a more detailed account is given elsewhere.[18] Microscopic tracks are defined in a UHV sputtered niobium-copper bilayer (125 nm Nb on 75 nm Cu) by photolithography and lift-off on an oxidized Si substrate. The sample is wire bonded to a custom-built chip carrier and loaded in the FIB system (FEI 200 xP). A 50 nm trench is milled across a track using a 30 keV 4 pA Ga^+ ion beam. Whilst the trench milling takes place, the resistance of the track is measured *in situ*;[19] assuming a rectangular trench profile, a simple algorithm can be used to determine the milling depth. Transmission electron microscopy (TEM) studies confirm that for an aspect ratio up to 2.5 the profile remains rectangular (Fig. 2). At high aspect ratio, material is resputtered in the bottom of the trench leading to a tapered trench profile. We have shown that, with a thick Cu layer (thicker than the dirty limit coherence length) $\simeq 75$ nm, junctions with nonhysteretic resistively-shunted junction (RSJ) type current–voltage (I-V) characteristics at 4.2 K can be obtained over a range of milling depths (from 60% through the Nb thickness). The critical current I_C is controlled by the remaining Nb thickness.

B. Corbino geometry junction fabrication

As before, a microscopic track layout is defined by lift-off patterning of the sputtered bilayer. The track layout contains a main track of 8, 7, and 6 μm width sections tapped by voltage/current lines. The milling depth of a 50 nm wide trench on a 4 pA FIB beam current is calibrated on a test track using the *in situ* resistance measurement. Circular trenches (radius $r=2.5\ \mu$m, various depths 60–100 % through Nb thickness) are then milled in the main track.

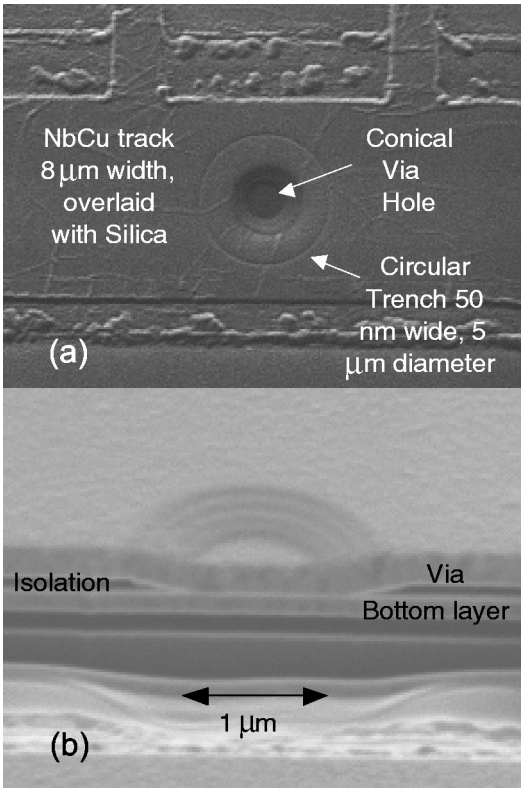

FIG. 3. (a) FIB image of device after via hole milling. (b) Sectioned conical via viewed at 45° tilt in the FIB.

Isolation cuts are milled in the main track to separate the individual devices using a large beam current (70 pA). After further lift-off patterning, a silica isolation layer (thickness 250 nm) is deposited by RF sputtering over the region of interest. The sample is then returned to the FIB system and via hole milled onto the central island of each junction. In the FIB, milling depth per unit area through an insulating layer can be calibrated by measuring the sample stage current; a jump is observed when the insulating layer is breached. Straight-sided via holes were found to give poor via filling when the final metallization layer was deposited, leading to a considerable shunt resistance in early devices.[20] The perfected via hole procedure is as follows: a sequence of concentric circles is milled (1.25 to 0.75 μm radius) to create a conical hole 80% of the way through the insulator. After a final lift-off patterning stage, the sample is transferred to a combined Ar milling/ dc magnetron sputtering system. The final (Ga-implanted) insulating layer is removed by Ar ion milling and a Nb-Au (30 nm Nb, 200 nm Au) layer is deposited without breaking vacuum. Figure 3 (a) is an FIB image of a device at the end of the via hole milling stage. Figure 3 (b) shows a conical via (no junction barrier defined) sectioned and viewed at 45° tilt in the FIB.

III. RESULTS

A. Measurements at 4.2 K

We are now routinely able to produce Corbino geometry junctions with comparable critical current densities to the

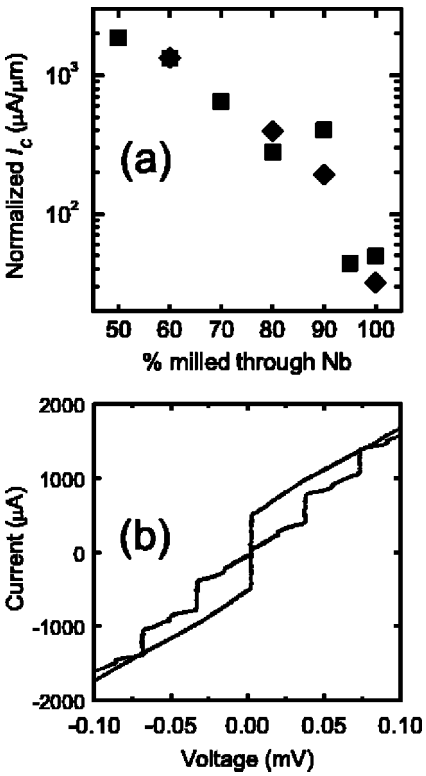

FIG. 4. (a) Critical current at 4.2 K normalized to barrier width versus milling depth for planar SNS (squares) and Corbino geometry SNS junctions (diamonds). (b) Current-voltage characteristic of Corbino geometry junction with and without microwaves at 4.2 K. The microwave frequency is 17 GHz; the series resistance due to the via contact is less than 1 mΩ.

planar SNS junctions previously fabricated. Figure 4(a) shows a comparison plot of normalized critical current versus milling depth through the Nb layer for planar SNS and Corbino geometry devices. Given that the uncertainty in the milling depth is $\simeq 5\%$, the correspondence between the two datasets is extremely good. Figure 4 (b) shows the current-voltage (I-V) characteristic of a Corbino geometry junction at 4.2 K with and without applied microwave radiation. The I-V characteristic without microwaves is nonhysteric and approximately RSJ type. Series resistance due to the via contact is minimal. There is a strong microwave response: the critical current can be completely suppressed indicating a pure Josephson current and strong Shapiro steps are observed; half integer steps (a common feature of planar SNS devices[21]) are also evident.

As discussed in Sec. I, a distinctive magnetic-field response is expected for this type of device. Figure 5 shows the response in the critical current I_C of a high critical current Corbino geometry junction (5 μm diameter junction in 8 μm width track) to a changing perpendicular magnetic field at 4.2 K. Measurements were taken with a mumetal shielded dip probe in a He bath. Current-biased measurements were made of the I-V characteristic at each value of field; the value of I_C was extracted using a voltage criterion.

The sample was cooled to 4.2 K in zero magnetic field. Magnetic field was then applied perpendicular to the plane of the sample via a calibrated Helmholtz pair. Sweeping the

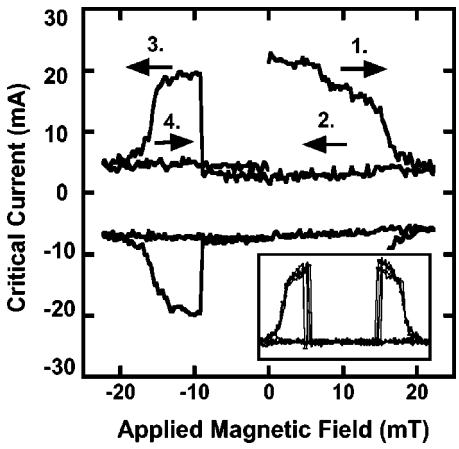

FIG. 5. Magnetic field response at 4.2 K of a 5 μm diameter junction in a 8 μm width track. The external field is swept from 0 to $+22$ mT to -22 mT to 0 (1. through 4.). Inset: this behavior is repeated over multiple cycles (the field range is again -22 mT to $+22$ mT).

external field over a small range (under 10 mT) leads to reversible perturbations in I_C, but no irreversible change. As shown in Fig. 5, if a large enough external field is applied (in excess of 15 mT), I_C is suppressed steeply and irreversibly. This can be identified as the entry of one quantum of flux ($\Phi_0 = h/2e$) into the junction barrier. Subsequently, when the external field is reduced back to zero I_C remains suppressed and the flux is trapped in the junction. As the field direction is reversed I_C reappears abruptly at $\simeq -8$ mT. At this point a flux quantum of opposite orientation enters the junction and annihilates the original trapped vortex. A second steep, but not abrupt, suppression of I_C occurs at $\simeq -15$ mT corresponding to the trapping of a flux quantum of negative polarity in the junction barrier. As illustrated in Fig. 5 (inset) this behavior can be repeated over multiple cycles, the flux entry/annihilation events occurring at almost identical fields (given the presence of electrical and thermal noise at 4.2 K). This dynamic response of the critical current to magnetic field is dependent on the exact configuration of the Meissner state in the superconductor; slightly different behavior can be observed in the same device each time it is heated and cooled through the superconducting transition.

A more reproducible way to identify the flux entry event is to *field cool* the device at set external field. In this case the screening currents that impede vortex entry in the dynamic $I_C(B)$ measurements are absent. There remains a minimum cooling field B_C above which vorticies can stably exist in the track.[22] This is approximately given by $B_C = \Phi_0 / w^2$, where w is the track width —i.e., $w \simeq$ mean vortex separation. For 8 μm track width we may expect vortex entry into the track above $\simeq 30$ μT. Results for a Corbino geometry junction (5 μm junction in a 8 μm track—junction of lower current density) are shown in Fig. 6. I_C is rapidly suppressed with cooling field of less than 100 μT, indicating vortex entry into the track in the region of the junction. However, conclusive evidence of flux trapping in the barrier itself is only observed at relatively high cooling fields (>2 mT). Quantized flux trapping in the barrier is identified by performing an $I_C(B)$ sweep at 4.2 K. If the field was swept first in the

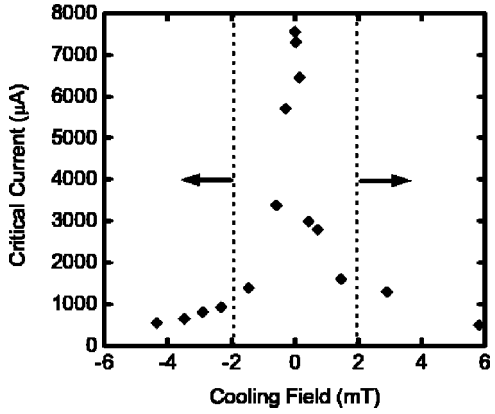

FIG. 6. Field-cooled measurements of critical current. Irreversible flux trapping in the junction barrier occurs at an external flux density of magnitude >2 mT as indicated.

same direction as the cooling field, no change should be expected (I_C remains suppressed). An annihilation event is then expected when the external field direction is reversed. A field of 2.5 mT corresponds to a mean vortex separation of $\simeq 1$ μm. Hence in summary, this measurement shows that flux is entering the film at low cooling field, but being pinned as Abrikosov vorticies in the region of the junction, rather than as a Josephson vortex in the barrier itself. Polycrystalline thin film Nb certainly contains a high density of pinning sites and this situation is exacerbated by 30 kV Ga^+ ion implantation during the device fabrication process. The via contact, in particular, is liable to contain a large concentration of pinning sites.

We have fabricated and measured devices consisting of 5 μm diameter trenches in tracks of 8, 7, and 6 μm width. With the narrowest tracks, the minimum separation between the junction and the outer edge of the superconductor is only 500 nm. We hence enter the limit where the superconductor surrounding the junction barrier is of the order of the effective London penetration depth λ_p at its narrowest point. Figure 7 shows $I_C(B)$ at 4.2 K for a 5 μm diameter junction in a 6 μm width track. The critical current is now suppressed in a series of jumps. As the field is reduced and swept in the negative direction, critical current reappears incrementally, before another series of suppression events. As in Fig. 5, this behavior was repeatable over a large number of cycles.

This behavior strongly suggests that flux entry is now occuring in units of less than $h/2e$. The condition for fluxoid quantization in the London theory is

$$\oint (\underline{A}+\Lambda \underline{J_S})\cdot \underline{dl} = \frac{\hbar}{2e} 2\pi n, \qquad (1)$$

where A is the magnetic vector potential, Λ is the London parameter, and J_S is the screening current density.[23] To achieve magnetic flux quantization in units of $\Phi_0 = h/2e$, J_S must be zero. Close the edge of a superconductor it is no longer possible to choose an integration contour such that $J_S = 0$. In a bulk superconductor, this effect is only expected to occur over very short length scales, but in the case of a thin superconducting film (thickness $<$ London penetration depth) it has been shown[24,25] that flux quantization occurs in units of less than $h/2e$ over mesoscopic distances from an edge.

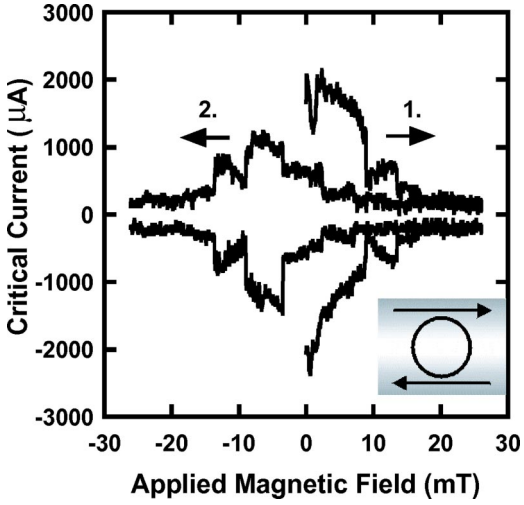

FIG. 7. Critical current versus magnetic-field response of a 5 μm diameter junction in a 6 μm track. The external field is swept from 0 to $+25$ mT then -25 mT. Inset: schematic of geometry. Flux quantization is not achieved if screening currents flowing in the edge of the film overlap with the junction.

B. Modeling the approach of a single vortex to the junction

We have developed a theoretical model of the device response to the approach of a single vortex. First consider an Abrikosov vortex in a semi-infinite thin film. As the interface is approached the flux on the vortex is reduced.[24] The relevant penetration depth is $\lambda_p = (\lambda_L)^2/t$, where λ_L is the bulk London penetration depth and t is the film thickness (λ_p is often referred to as Pearl's penetration depth[26]). In this case at 4.2 K, $\lambda_p \simeq 100$ nm. The distance between the vortex core and the edge of the film is a. The inset of Fig. 8 shows a

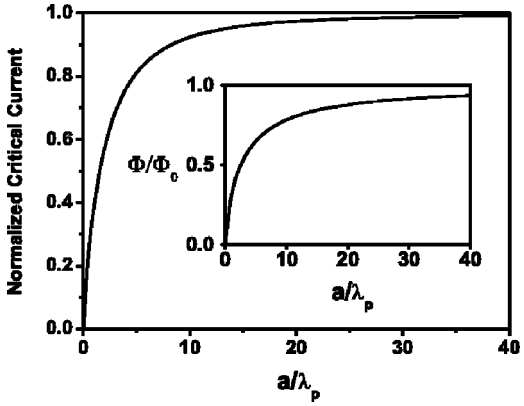

FIG. 8. The simulated critical current response of a Corbino geometry junction to the approach of a single vortex. The junction is assumed to be embedded in an *infinite* thin film. The minimium separation of the vortex from the junction barrier a is normalized to the effective London penetration depth λ_p. Inset: the underlying premiss of this simulation is that the flux associated with a vortex trapped in a superconducting thin-film Φ/Φ_0 is reduced over mesoscopic distances (Ref. 24).

simulation (after Ref. 24) of how the flux associated with the vortex is reduced as the surface is approached. Note that this predicts a significant reduction in the flux associated with the vortex is over distance of microns: at $a=10\lambda_p=1\ \mu$m, $\Phi/\Phi_0=0.8$.

The same approach can be applied to the approach of a vortex to a hole in an infinite superconducting sheet. As the vortex approaches the hole, the flux lost by the vortex must be transferred to the hole. Similarly, if we have a Corbino geometry junction embedded in an infinite superconducting sheet, the flux lost by the approaching vortex must migrate to the junction barrier. In the short junction limit ($\lambda_J \gg 2\pi r \gg \lambda_p$), we can assume that this flux is uniformly distributed in the junction barrier. The effect on the phase difference around the junction barrier due to the approaching vortex is illustrated in Fig. 9. The phase varies linearly with θ due to the even distribution of flux in the junction barrier. The overall change in phase with one revolution must be 2π, therefore at θ_{Vortex} there is a discontinuity. When the vortex enters the junction the flux in the junction is equal to Φ_0, so the discontinuity vanishes. In the short junction limit, it is straightforward to calculate the variation in junction I_C with vortex separation a,

$$I_C \propto \sin[2\pi.\Phi_h(a)/\Phi_0+\phi_0]. \tag{2}$$

The flux in the junction is simply the flux lost by the approaching vortex: $\Phi_h(a)=\Phi_0-\Phi$. Maximizing with respect to ϕ_0, we obtain the result of Fig. 8. The simulation of Fig. 8 suggests that critical current I_C will be suppressed steeply, but not abruptly, as a vortex approaches the junction. This is quite similar to the suppression of I_C that we see in the data (Fig. 5). Realistically in the $I_C(B)$ measurements performed, I_C is responding to the approach of a number of Abrikosov vortices via pinning sites in the superconducting film, which move inwards under the action of screening currents. These screening currents, in turn, are changing in response to the variation of external magnetic field. The first vortex to reach the junction is then trapped as a Josephson vortex in the barrier. The result of Fig. 7 can be explained in the same fashion. The minimum distance from the junction barrier to the edge of the superconductor is only 500 nm$\simeq 5\lambda_p$. From the prediction of Fig. 8 (inset), at $a=5\lambda_p$, $\Phi/\Phi_0\simeq 0.6$. Hence I_C is suppressed in a series of steps as a succession of vortices, each carrying an overall flux less than $h/2e$, enter the junction.

It should be noted that the junctions used in this investigation are in the long junction limit at 4.2 K, which explains why I_C is small but not equal to zero when flux is trapped. This is clear from the comparison with planar SNS junctions: as Fig. 4(a) shows, the critical current per unit barrier width scales with milling depth in the same way in both Corbino geometry and planar SNS junctions. By fabricating planar SNS junctions of different widths and equal trench depths, we have observed the transition from short to long junction behavior. The Josephson penetration depth $\lambda_J\simeq 0.5\ \mu$m at 4.2 K. This value should apply equally well to the Corbino geometry devices: $\lambda_J<1\ \mu$m as compared to an overall barrier circumference w of 15.7 μm. The flux in the junction will then be confined on the length scale of λ_J. Simulations of Abrikosov vortex approach to a long junction are more challenging, but qualitatively may be expected to yield a similar result in the Corbino geometry case as that illustrated in Fig. 8.

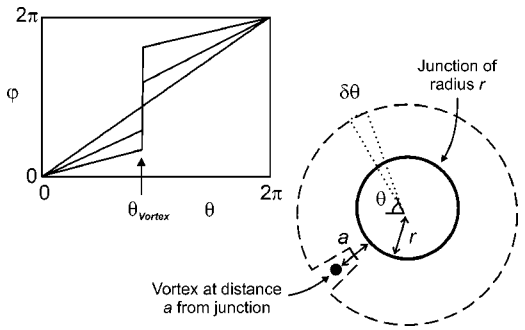

FIG. 9. Calculating the critical current response of the Corbino geometry junction to the approach of a single vortex. At separation a the flux associated with the vortex is $\Phi(a)$; the remainder of the flux, $\Phi_0-\Phi(a)$ is evenly distributed in the junction barrier (the short junction limit is assumed). Hence integrating over angle θ using the contour indicated, we arrive at the variation of phase difference across the junction $\phi(\theta)$. For $a>0$, ϕ varies linearly with θ, except for a discontinuity at θ_{Vortex}, to arrive at an overall phase difference of 2π.

It is clear that the approach of a second vortex will not lead to a significant change in the critical current I_C—there may be a small reappearance of I_C when the vortex is very close. When the external field direction is reversed, a more dramatic result can be expected—antivorticies penetrate the film. The vortex trapped in the junction and the antivortex experience an attractive force, leading an abrupt annihilation. This is evinced in the $I_C(B)$ characteristic as a rapid reappearance of I_C. This is indeed what is seen in Fig. 5 when the applied field is reversed to $\simeq -8$ mT. Again in Fig. 7, as both vortices and antivortices carry a flux of less than $h/2e$, with negative field I_C returns in a series of steps.

By considering the approach of an individual vortex to the junction, we have succeeded in providing a satisfactory explanation for the most striking behavior observed in these devices, namely, the abrupt suppression and reappearance of I_C. Secondary features observed in the $I_C(B)$ measurements taken, such as the reversible perturbation of I_C at low fields and asymmetry in the $I_C(B)$ traces for devices where the junction is offset from the axis of the track, can be explained by considering the I_C response to screening currents in the edge of the track and self-field of the bias current. Simulations have been carried out based on these considerations with fair success.[27]

IV. DISCUSSION

The electrical measurements presented above can be best explained in terms of the motion of individual vorticies. The movement of vorticies in the vicinity of the junction is inferred from changes in the junction critical current. A fascinating extension of this experiment would be to *image* the vortex distribution whilst measuring the junction critical current. There are currently various techniques available to im-

age individual vortices in superconducting structures. Scanning Hall probe microscopy[28] and scanning SQUID microscopy[29] allow individual vortices to be imaged (via magnetic fields and flux, respectively) to $\sim 1\ \mu$m resolution. An alternative technique that has been applied successfully to Josephson junctions is low-temperature scanning electron microscopy.[30] In this case the surface of the sample is perturbed by the electron beam, allowing current density through the junction to be imaged and the presence of trapped vortices to be deduced. Furthermore the electron beam provides a means of manipulating vortices in a superconducting film.[31] In priniciple, the devices used in this investigation should be suitable for such experiments. They are sufficiently large (radius $r=2.5\ \mu$m) and although the junction barrier is overlaid with material, the upper (via) layer is not superconducting and should be transparent to the technique.

The dependence of junction properties on the effective magnetic-field distribution around the barrier has interesting implications: consider a Corbino junction embedded in a microscopic track (exactly as in the devices of Sec. III) with a flux quantum trapped in the junction barrier (extent of vortex $\sim\lambda_J$, the Josephson penetration depth $\ll 2\pi r$). If an external magnetic field is applied perpendicular to the plane of the film, screening currents flow in the edge of the track, decaying with the effective penetration depth λ_p. This creates a field distribution H_1 in the barrier, which is inhomogeneous with angle θ. Taking $\theta=0$ on the track axis, H_1 will be maximum close to the track edges ($\theta=\pi/2$ or $3\pi/2$). The overall field energy is $\alpha[H_1(\theta)+H_{Vortex}]^2$, so the potential energy takes the same form as $H_1(\theta)$. Hence the trapped vortex will be located at $\theta=0$ or π i.e., in double-well potential. A similar situation is commonly observed in imaging studies of vortices in microscopic superconducting tracks: the vortices are typically confined along the track axis, as far from the edges possible.[32] For a vortex trapped in the barrier of a Corbino geometry junction, the depth of the potential can be varied by the magnitude of the external field and, since λ_J is strongly temperature dependent, the shape of the potential is modified by the temperature. If a bias current is applied through the junction, the vortex can be driven between minima. Double-well potentials in heart shaped annular junctions have been proposed as the basis of a qubit, the basic element of a quantum computer.[33] It is proposed that at sufficiently low temperatures, macroscopic quantum tunneling[34] of fluxons will occur. In our case, we have an overdamped SNS junction as opposed to an underdamped SIS junction (this implies a quality factor 10^6 smaller), which means quantum effects persist over impracticably short timescales and the trapped vortex behaves as a classical object. To raise the quality factor of our Corbino geometry junctions and enter the quantum regime we could capacitively shunt the existing junctions or employ in-plane SIS ramp junctions.

It has recently been pointed out[14,17] that the appearance of a Berry phase as a vortex is driven around a circular junction barrier should lead to a disturbance of the current distribution and a variation in the driving force on the vortex. This should be expressed as a measurable variation in the *I-V* characteristics of the junction at low (mK) temperatures. Common annular SIS junctions are unsuited to this type of experiment because the geometry is incorrect. We have succeeded in creating a device in the ideal geometry. A further consideration which has to be taken into account is that a clean SNS barrier is required (coherence length in *N* layer longer than overall barrier width). At present, our junctions are in the dirty limit[18]—that is to say, the coherence length in the junction barrier is shorter than the barrier width.[35] The use of epitaxial Cu-Nb bilayers or the use of a two-dimensional electron gas as the *N* layer would significantly raise the coherence length in the junction barrier, enabling the fabrication of a clean limit Corbino geometry SNS junction.

V. CONCLUSIONS

We have succeeded in realizing the first Corbino geometry SNS junction. In this paper, we have focused primarily on measurement of critical current in response to an applied magnetic field at 4.2 K. As the junction barrier is embedded in a superconducting strip, magnetic flux can only enter as quantized units. A dynamic measurement of critical current as external field is varied reveals abrupt suppression/reappearance of critical current, corresponding to flux entry/annihilation in the junction barrier. When the superconducting region surrounding the barrier is sufficiently thin, the suppression/reappearance occurs in a series of steps suggesting incomplete flux quantization. We have developed a model for the critical current response of the junction to external field up to the point of irreversible flux entry into the barrier. These considerations lead us to believe that a trapped vortex is confined in a double potential well in this device geometry. We have demonstrated that studies of this Josephson junction geometry are now technologically feasible and hope that this report will stimulate further experimental and theoretical studies.

ACKNOWLEDGMENTS

This work was supported by the U.K. Engineering and Physical Sciences Research Council (EPSRC). R.H.H. would like to thank Dr. Stephen Lloyd for his assistance in the TEM studies, Dr. Sam Benz and Dr. Paul Dresselhaus for providing the bilayer films used in this work.

*Present address: Electromagnetic Technology Division, National Institute of Standards and Technology, 325 Broadway, Boulder, CO 80303, USA. Electronic mail: hadfield@boulder.nist.gov

[1] D.R. Tilley, Phys. Lett. **20**, 117 (1966).

[2] O.D. Cheishvili, Fiz. Tverd. Tela (Leningrad) **11**, 185 (1969) [Sov. Phys. Solid State **11**, 138 (1969)].

[3] M.D. Sherrill and M. Bhushan, Phys. Rev. B **19**, 1463 (1979).

[4] M. Kuwada, Y. Onodera, and Y. Sawada, Phys. Rev. B **27**, 5486 (1983).

[5] M.D. Sherrill, Phys. Lett. **82A**, 191 (1981).

[6] A. Davidson, B. Dueholm, B. Kryger, and N.F. Pedersen, Phys. Rev. Lett. **55**, 2059 (1985).

[7] A.V. Ustinov, Physica D **123**, 315 (1998).
[8] A. Wallraff, Doctoral thesis, 2001, Friedrich-Alexander University, Erlangen-Nuremberg, Germany.
[9] C. Nappi, Phys. Rev. B **55**, 82 (1997).
[10] R. Cristiano, M.P. Lisitskii, C. Nappi, and A. Barone, Phys. Rev. B **62**, 8683 (2000).
[11] E. Kavoussanaki, R. Monaco, and R.J. Rivers, Phys. Rev. Lett. **85**, 3452 (2000).
[12] C. Nappi, R. Cristiano, M.P. Lissitski, R. Monaco, and A. Barone, Physica C **367**, 241 (2002).
[13] M.V. Berry, Proc. R. Soc. London, Ser. A **392**, 45 (1984).
[14] F. Gaitan, Phys. Rev. B **63**, 104511 (2001).
[15] O.M. Corbino, Nuovo Cimento **1**, 397 (1911); Phys. Z. **12**, 561 (1911).
[16] A. Barone and G. Paterno, *Physics and Applications of the Josephson Effect* (Wiley, New York, 1982).
[17] V. Plerou and F. Gaitan, Phys. Rev. B **63**, 104512 (2001).
[18] R.H. Hadfield, G. Burnell, W.E. Booij, S.J. Lloyd, R.W. Moseley, and M.G. Blamire, IEEE Trans. Appl. Supercond. **11**, 1126 (2001).
[19] A. Latif, W.E. Booij, J.H. Durrell, and M.G. Blamire, J. Vac. Sci. Technol. B **18**, 761 (2000).
[20] R.H. Hadfield, G. Burnell, P.K. Grimes, D.-J. Kang, and M.G. Blamire, Physica C **367**, 267 (2002).
[21] P. Dubos, H. Courtois, O. Buisson, and B. Pannetier, Phys. Rev. Lett. **87**, 206801 (2001).
[22] J.R. Clem (unpublished).
[23] M. Tinkham, *Introduction to Superconductivity*, 2nd ed. (McGraw-Hill, New York, 1996).
[24] V.G. Kogan, Phys. Rev. B **49**, 15 874 (1994).
[25] A.K. Geim, S.V. Dubonos, I.V. Grigorieva, K.S. Novoselov, and V.A. Schweigert, Nature (London) **407**, 55 (2000).
[26] J. Pearl, Appl. Phys. Lett. **5**, 65 (1965).
[27] R.H. Hadfield, Ph. D thesis, 2002, University of Cambridge, UK.
[28] S.J. Bending, A.N. Grigorenko, G.D. Howells, R.G. Humphreys, J. Bekaet, M. Van Bael, K. Temst, L. Van Look, V.V. Moschalkov, T. Bruynseraede, and G. Borghs, Physica C **981**, 341 (2000).
[29] J.R. Kirtley, C.C. Tsuei, J.Z. Sun, C.C. Chi, L.S. Yujahnes, A. Gupta, M. Rupp, and M.B. Ketchen, J. Supercond. **8**, 487 (1995).
[30] R. Gross and D. Koelle, Rep. Prog. Phys. **57**, 651 (1994).
[31] A.V. Ustinov, T. Doderer, B. Mayer, R.P. Huebener, A.A. Golubov, and V.A. Oboznov, Phys. Rev. B **47**, 944 (1994).
[32] S. Field and J.M. Martinis (unpublished).
[33] A. Wallraff, Yu. Koval, M. Levitchev, M.V. Fistul, and A.V. Ustinov, J. Low Temp. Phys. **118**, 543 (2000).
[34] A.O. Caldiera and A.J. Leggett, Phys. Rev. Lett. **46**, 211 (1981).
[35] K.A. Delin and A.W. Kleinsasser, Supercond. Sci. Technol. **9**, 227 (1996).